2013 IEEE/RSJ International Conference on
Intelligent Robots and Systems (IROS)
November 3-7, 2013. Tokyo, Japan

Hemispherical Net-structure Proximity Sensor Detecting Azimuth and Elevation for Guide Dog Robot

Hikaru Arita*, Yosuke Suzuki*, Hironori Ogawa**,
Kazuteru Tobita**, Makoto Shimojo*

***Abstract*— We have developed a net-structure proximity sensor that detects the azimuth and elevation to a nearby object. This information can be used by robots to avoid obstacles or to respond to human behavior. We propose detection principles where the azimuth is detected by arranging two one-dimensional net-structure proximity sensors along orthogonal axes, and the elevation is detected by arranging two one-dimensional net-structure proximity sensors in a stacked ring. We also experimentally demonstrate the feasibility of these detection principles. The experimental result shows the sensor can detect azimuth at all peripheral angles and elevation from side to top up.**

I. INTRODUCTION

The coexistence of humans and robots has become an important topic in robotics in recent years. Robots were first used in limited environments such as manufacturing plants, but owing to technological advances, usage environments are broadening. Presently, the use of robots to perform assistive tasks alongside humans is drawing increased attention, but success will rely upon finding ways for robots and humans to communicate. In particular, robots will necessarily be equipped with responsive sensing apparatuses that can interpret human body language in the way that humans can.

Here is an example of the NWR002 (Fig. 1) [1], an NSK-developed robot that can lead others around obstacles. The NWR002 is being developed with the goal of creating guide dog–like functionality.

For the robot to fully implement its guidance features, users must grip a handle that serves as a control. As a tool being designed for the blind, however, grasping a handle can be a nontrivial task. One solution to this problem is incorporation into the grip of a sensor that can detect the user's hand without direct contact. Once the orientation of the user's hand is obtained, the grip could follow it and smoothly approach until contact is made. To realize this, the sensor must be suitable for incorporation into a grip, and information must not be lost from the time of approach to contact.

There has been previous research concerning methods for applying directional information of objects as seen from the robot's point of view [2]–[5], as well of proposed methods for determining directional information [6]–[9]. These methods, however, were not developed with the goal of aiding contact through approach of an irregularly shaped sensor, as in this case.

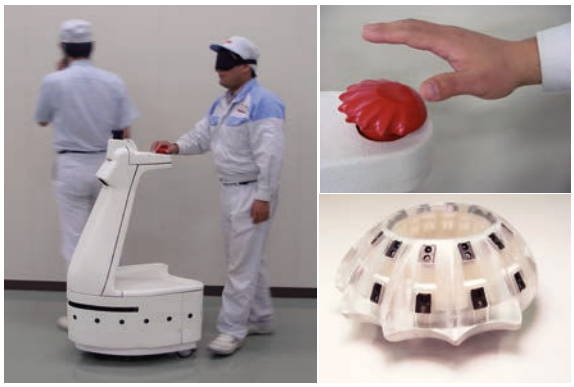

Fig. 1. NWR002 developed by NSK Ltd. for leading the blinds around obstacles: Left figure shows its exterior. The grip used for the control is shown in top-right figure. In bottom-right figure, the sensor developed in this paper is incorporated into the grip.

Our research focuses on the development of a net-structure proximity sensor that excels at close-range sensing from contact to several tens of centimeters. The net-structure proximity sensor uses a photoreflector comprising a light-emitting diode (LED) and a phototransistor as its detection element. Phototransistors capture reflected infrared light from the LED, and the position of a proximal object is inferred according to the photocurrent distribution. A primary feature of this sensor is that object position inference can be performed using analog computation by a resistor network circuit. Serially reading the response levels of individual photosensitive elements, as in the case of a general-purpose CCD image, requires complex wiring due to the number of elements and the size of the unit. Moreover, data acquisition and processing times are long. When using a net-structure proximity sensor, on the other hand, high-speed response and simple wiring requirements are retained, even when the number of elements is increased to accommodate the form of the installation surface. This is an important consideration for application to a complex shape, such as a grip designed to fit the human hand.

In previous research, Hasegawa et al. [11] demonstrated methods for establishing a firm grip on objects by means of a net-structure proximity sensor and haptic sensors, and Terada et al. [12] developed a net-structure proximity sensor capable of full-periphery sensing. Because the sensor forms a uniform grid of resistance values, the obtained position

*Mechanical Engineering and Intelligent Systems, The University of Electro-Communications, 1-5-1 Chofugaoka, Chofu-shi, Tokyo 182-8585, Japan

**Emerging Technology Research Center, Mechatronics Technology Development Center, NSK Ltd. 1-5-50, Kugenuma-shinmei, Fujisawa-shi, Kanagawa 251-8501, Japan

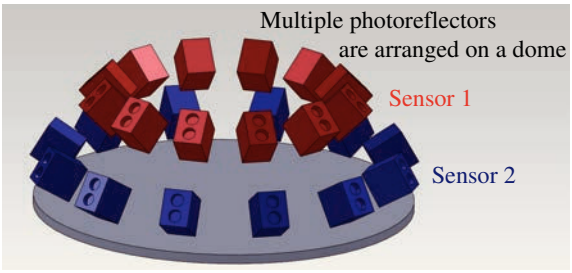

Fig. 2. The dome sensor is formed from two circular sensor. The sensors are placed in two layers in the height direction.

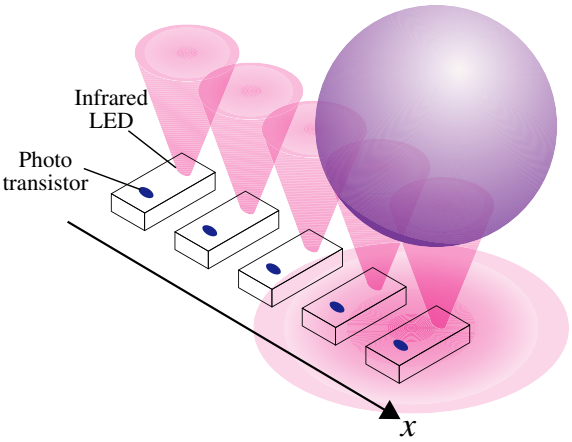

Fig. 3. Overview of the one-dimensional net-structure proximity sensor: The lights from the infrared LEDs reflect off of objects proximal to the sensor, and are collected in the phototransistors. This causes photocurrent to flow, generating the photocurrent distribution that corresponds to the distribution of reflected light at the phototransistor surface.

information can be described in Cartesian coordinates.

In this paper, we continue the discussion of how to form the resistance network. In particular, we demonstrate how methods of connecting detection elements in the resistor network, as well as the resistance values of the constituent resistors, can provide output features suited to the target application. As an example, we describe a net-structure proximity sensor suited to the acquisition of object positions in polar coordinates, namely their azimuth and elevation.

II. Sensor Design and Detection Principles

We refer to the developed azimuth and elevation proximity detector as a dome sensor. The dome sensor is formed from two round, one-dimensional net-structure proximity sensors(Fig.2). Each of the two sensors can obtain one-dimensional positional coordinates. Azimuth is determined by orthogonally aligning each sensor's coordinate axis. Each sensor can also measure the distance to target objects. Elevation is determined by placing sensors in two layers in the height direction, and performing distance detection with each.

A. The one-dimensional net-structure proximity sensor

This section describes the one-dimensional net-structure proximity sensor, which is the most fundamental part of the

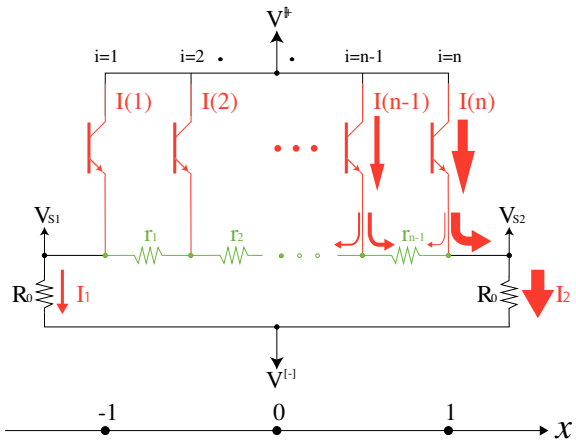

Fig. 4. Circuit diagram of the one-dimensional net-structure proximity sensor: When a photocurrent occurs at the element, the currents diverges and flows to the negative supply $V^{[-]}$.

dome sensor. Figure 3 and 4 show the overview and the circuit structure.

The one-dimensional net-structure proximity sensor consists of a resistor network and string of n photoreflectors (called elements below) in a given direction, defined as the x-axis for convenience. The resistor network is formed from $n-1$ internal resistors $r_i (i = 1 \sim n-1)$ between the elements, and an external resistors R_0 that connect the terminals on both ends V_{S1}, V_{S2} and a negative supply $V^{[-]}$.

Light from an infrared LED reflects off of objects proximal to the sensor, and is collected in the phototransistor. This causes photocurrent to flow, generating a photocurrent distribution that corresponds to the distribution of reflected light at the phototransistor surface. When a photocurrent I_i occurs at the ith element, the currents flowing between terminals V_{S1} and V_{S2} are described as follows:

$$I_{i1} = \frac{\sum_{k=i}^{n-1} r_k + R_0}{\sum_{k=1}^{n-1} r_k + 2R_0} I_i, \quad I_{i2} = \frac{\sum_{k=1}^{i-1} r_k + R_0}{\sum_{k=1}^{n-1} r_k + 2R_0} I_i \tag{1}$$

The difference between the currents flowing to terminals V_{S1} and V_{S2} is therefore

$$I_{i1} - I_{i2} = \frac{\sum_{k=i}^{n-1} r_k - \sum_{k=0}^{i-1} r_k}{\sum_{k=1}^{n-1} r_k + 2R_0} I_i \tag{2}$$

The numerator in Eq. (2) is the product of the resistance at each element from the center of the serially connected resistor network with the current flowing through it, and represents the one-dimensional moment of the current at the center. When a photocurrent distribution arises in the resistor network, the abovementioned phenomenon will occur in all elements. The photocurrents will therefore flow together, and

the following equations will hold:

$$\sum_{i=1}^{n-1}(I_{i1}-I_{i2}) = \sum_{i=1}^{n-1} I_i \frac{\sum_{k=i}^{n-1} r_k - \sum_{k=1}^{i-1} r_k}{\sum_{k=1}^{n-1} r_k + 2R_0} = \frac{V_{S1}-V_{S2}}{R_0} \quad (3)$$

$$\sum_{i=1}^{n-1} I_i = I_{all} = \frac{V_{S1}+V_{S2}-2V^{[-]}}{R_0} \quad (4)$$

Removing the one-dimensional moment calculated by Eq. (3) from the overall current I_{all} calculated by Eq. (4) allows identification of the photocurrent distribution's central point. Here, the range of possible acquired values are changed according to the sensor configuration. To improve ease-of-use, Eq. (5) is used on the one-dimensional net-structure proximity sensor output to normalize the center point to the range $[-1,1]$. Here, positioning output characteristics can be determined by determining internal resistance values.

$$x_c = -\left(1+\frac{2R_0}{\sum_{i=1}^{n-1} r_i}\right)\left(\frac{V_{S1}-V_{S2}}{V_{S1}+V_{S2}-2V^{[-]}}\right) \quad (5)$$

When the amount of reflected light gathered by the phototransistor changes according to the distance between the sensor and the proximal object, the total current through the resistor network also changes. This allows estimation of the approximate distance to the object by using Eq. (4) to obtain the total current through the resistor network.

B. Azimuth detection

The azimuthal orientation of the object is detected by deriving cosine and sine values from the one-dimensional net-structure proximity sensor output. Figure 5(a) shows the circular arrangement of the sensor elements of the one-dimensional sensor described in the previous section. The internal resistors in the proximity sensors are set so that positioning output forms a cosine wave when an object goes around the sensor, as shown in Fig. 5(b). In the case where six elements are used (Fig. 5), the ratios of internal sensors will be $1:2:1$ in proportion to real-space positions. Two such circular one-dimensional net-structure proximity sensors are used, and are respectively called sensor 1 and sensor 2. As Fig. 6 shows, orthogonally orienting these sensors creates a 90° phase shift between them, allowing derivation of the sine value of the object's azimuth from the positioning output. The positioning output (x_{c1}, x_{c2}) obtained by the respective sensors and Eq. (6) can therefore uniquely determine the object's azimuth ϕ.

$$\phi = \begin{cases} \frac{\pi}{2} sgn(x_{c2}) & x_{c1} = 0 \\ \arctan\left(\frac{x_{c2}}{x_{c1}}\right) & x_{c1} > 0 \\ \pi sgn(x_{c2}) + \arctan\left(\frac{x_{c2}}{x_{c1}}\right) & x_{c1} < 0 \end{cases} \quad (6)$$

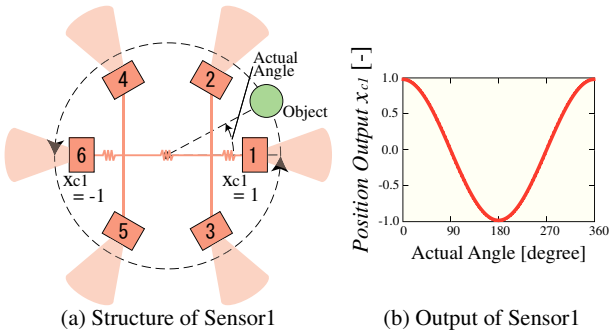

(a) Structure of Sensor1 (b) Output of Sensor1

Fig. 5. Structure and output of the circular one-dimensional net-structure proximity sensor: The positioning output forms a cosine wave for an object at the outer sensor periphery by the circular arrangement of the sensor elements and the internal resistors set.

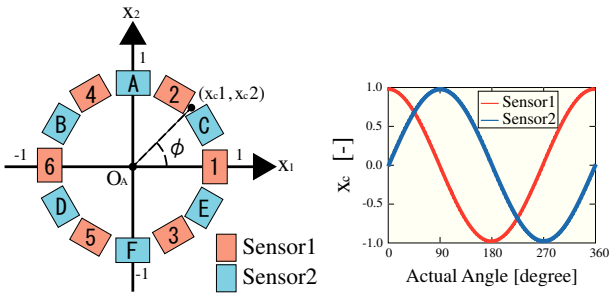

(a) Structure of Sensor (b) Output of Sensor

Fig. 6. Detection principle of azimuth: The orthogonally orienting two circular sensor allows derivation of the cosine and sine value of the object's azimuth from these positioning output.

C. Elevation detection

The two circular one-dimensional net-structure proximity sensors provide two distance outputs I_{all}, which are used to detect elevation without compromising the azimuth detection characteristics.

The two circular one-dimensional net-structure proximity sensors are stacked as shown in Fig. 7(a), (b). Because changes in elevation will change the distance to each of the sensors, the photocurrent flowing through sensors 1 and 2 will also change. Taking sensors 1 and 2 as single elements allows derivation of the elevation by considering them as a one-dimensional net-structure proximity sensor composed of two elements. Specifically, taking the distance output of the two sensors as I_{all1}, I_{all2} allows use of Eq. (7) to find the elevation output θ, normalized to the range [-1,1].

$$\theta = \frac{I_{all1}-I_{all2}}{I_{all1}+I_{all2}} \quad (7)$$

The normalized elevation output will be $+1$ if only sensor 1 is responding, -1 if only sensor 2 is responding, and continuously varying in the range $-1 < \theta < 1$ in the case where both sensors are responding. In this method, the range at which elevation can be detected depends on the tilt and positioning of the two stacked sensors. This allows the detection range to be set according to the intended purpose of the dome sensor.

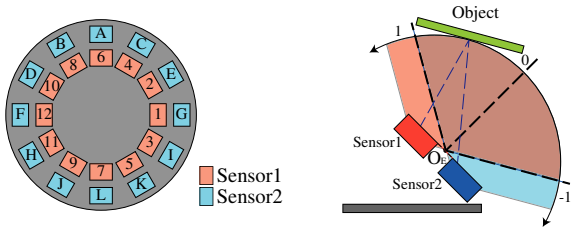

(a) Two-stage Arrangement (b) Side View

Fig. 7. Detection principle of elevation: (a) The two circular sensors are placed in two layers in the height direction. (b) The changes in elevation will change the distance to each of the sensors.

III. Prototyping and Experiments

A. Sensor prototype

When designing a dome sensor, it is possible to adjust element tilt and positioning according to the intended application. Here our aim is to develop a sensor incorporated into a grip that can detect and track a human hand, so we created a prototype device and investigated its detection characteristics. We identified the following design requirements:

- The elevation detection range must include the space to the sides and above the dome sensor.
- The sensor must be shaped to fit a human hand, based on a circular form with approximately 65 mm diameter.
- Detected objects would primarily be human palms, and thus an approximate planar square of 90×90 mm^2.

We varied the tilt of the elements in sensors 1 and 2 (α_{s1}, α_{s2}, respectively), and determined the element positioning best suited to our basic circular form. Because it would be difficult to create and test prototype sensors with a variety of tilt combinations, we used a net-structure proximity detection simulator developed in our lab. The simulator uses ray-tracing techniques to calculate levels of reflected infrared light, and simulates the output of a net-structure proximity sensor in an ideal environment. Figure 8 shows an overview of simulation operation. The angle at which the normalized elevation output is 0 is taken as 0°, and a 90 mm square object was moved through the space between −90° and 90° with respect to the origin of the elevation angle O_E. Table I shows the tilt combination investigated by this simulation.

TABLE I
Element Tilts

	α_{s1}	α_{s2}
Type 1	45 deg	30 deg
Type 2	45 deg	45 deg
Type 3	60 deg	45 deg

Figure 9 shows the simulation results.

As a result of the simulations, we found that the Type 1 combination has the most stable output fulfilling our design criteria that the output should increase monotonically in all range of the object angle β. Figure 10 shows the exterior of the dome sensor prototype implementing the selected element tilts. Twelve elements were evenly spaced along the dome sensor's periphery.

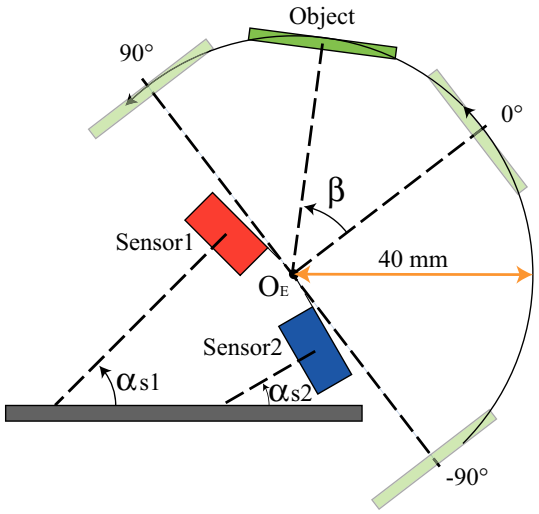

Fig. 8. Overview of simulation operation for determining element tilts: The angle at which the normalized elevation output is 0 is taken as 0°, and a 90 mm square object was moved through the space between −90° and 90° with respect to the origin of the elevation angle O_E.

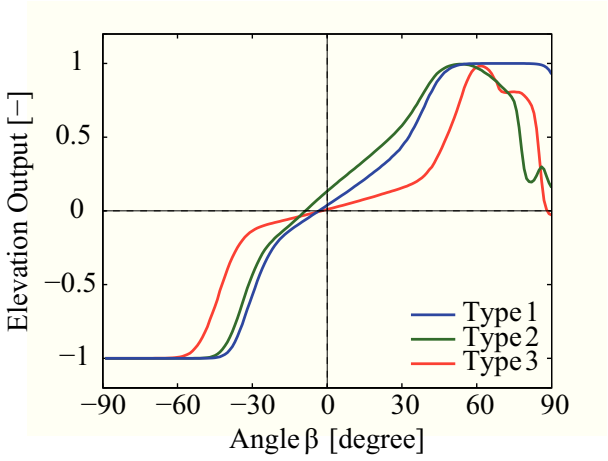

Fig. 9. Simulation results of elevation detection with three types element tilts shown in Table I

B. Detection characteristics

1) Azimuth detection characteristics: In this section, we examine the azimuth detection characteristic by an experiment with the prototyped dome sensor. The detection object was fixed, and output recorded as the dome sensor, which was affixed to a rotating stage, was rotated 360° in the positive ϕ direction in 1° increments. The distance between the dome sensor and the object was 30–60 mm.

Figure 11 shows the results of the experiment. Figure 12 shows actual azimuths and sensor output error.

Figure 11 indicates that the azimuth output of the sensor increased monotonically with increasing azimuth of the object. Because the object azimuth can be uniquely determined from the sensor output, this indicates successful detection of

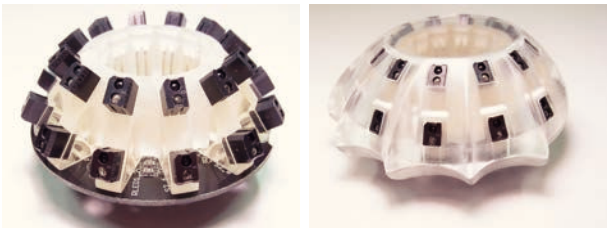

Fig. 10. Dome sensor: Right figure shows the exterior of the dome sensor prototype implementing the selected element tilts. Left figure shows the dome sensor is incorporated into the grip.

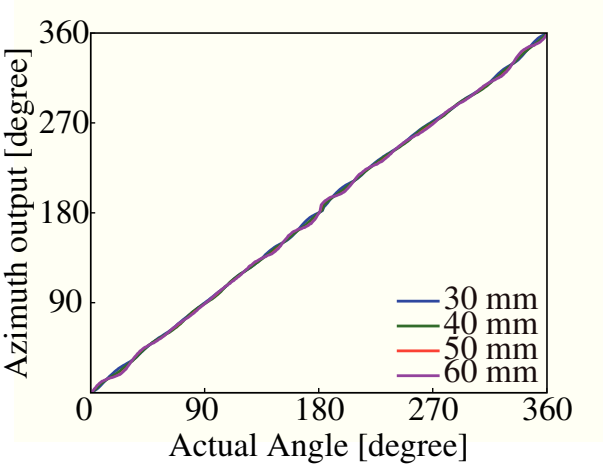

Fig. 11. Experimental results with changing the distance of 30–60 mm

the azimuth. Because azimuth output is always continuous, azimuth detection is possible over the entire 360° range.

Figure 12 indicates that azimuth detection error was within approximately ±5°. Detection error increased, however, in the 180–240° range. Considering that the same deviation occurs at the same position when the distance is changed, and that this deviation does not occur at other detection positions, we attribute this deviation to individual differences in the elements. Such error due to individual differences in the elements can be reduced by increasing the number of detection elements and treating multiple elements operating in parallel as a single element.

2) Elevation detection characteristics: In this section, we evaluate the elevation detection characteristic of the sensor. The detection object was fixed to a jig, which rotated the object in 1° increments in the elevation range [0,90], from side to top of the sensor, around the dome sensor, which was affixed to a rotating stage. The distance between the dome sensor and the object was 30–60 mm.

Figure 13 shows the comparison of the experimental result and the simulation result at the distance of 30 mm, and Fig.14 shows the comparison of the experimental results with changing the distance.

Figure 13 indicates that within an elevation range [0,90] with respect to the object, sensor output decreases monotonically with decreasing elevation angle. There is approximately +3° shift between the experimental result and simulation result. We attribute this to the production error. When elevation angle gets close to 0° or 90°, the absolute value of elevation output becomes less than simulation result. This is because the response of the sensor away from the object is small, and the signal-to-noise ratio is weak. Thus, we attribute the decreasing of the absolute value to the effects of noise.

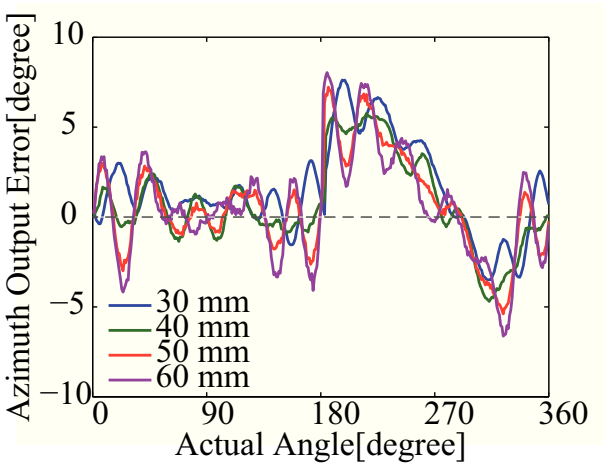

Fig. 12. Sensor output error with the actual azimuth of 0–360°

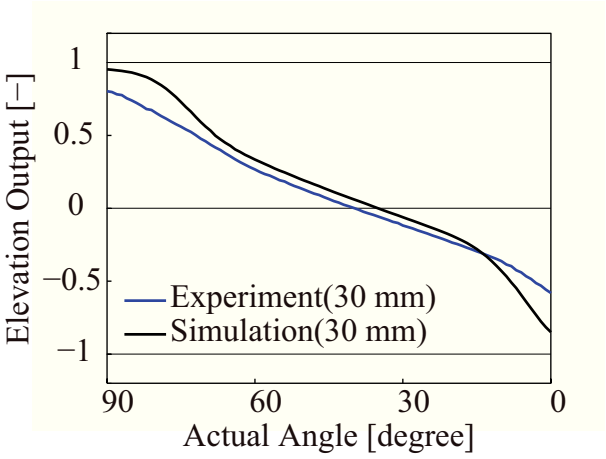

Fig. 13. Comparison of elevation output of the experimental result and the simulation result at the distance of 30 mm

Figure 14 indicates that the absolute value of elevation output near 0° or 90° increases with increasing distance. When the distance between the dome sensor and the object increases, the object's area accounting of detection range decreases, and so the object becomes easy to shift out of the range of sensor 1 or 2. Namely, the response of the sensor away from the object tends to decrease, and the absolute value decreases. The elevation output difference due to distance change decreases with decreasing distance between the sensor and the object. Thus, incorporating the dome sensor into the grip will allow tracking of hands by using the result in proximity as target.

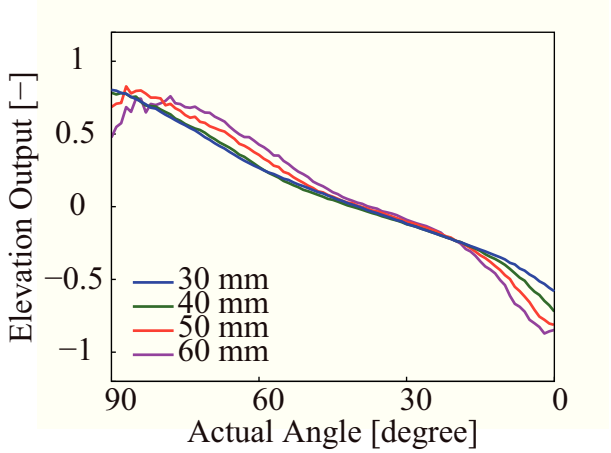

Fig. 14. Comparison of elevation output of the experimental results with changing the distance of 30–60 mm

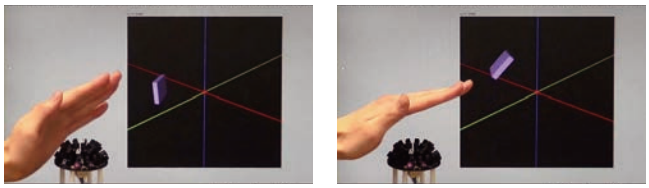

Fig. 15. Human-machine interface usage of the dome sensor: The dome sensor with the rapid response features can be applied to non-contact human interface applications, and results in a 3D representation of the object.

IV. Discussion

Experimentation indicates that the dome sensor can detect azimuth at all peripheral angles and elevation from side to top up to a distance of 60 mm. Azimuth detection error was retained to within $\pm 5^\circ$ for all distances, and elevation detection precision increased with lessened distance.

We expect that incorporating a dome sensor with above-mentioned characteristics into the grip of NWR002 will allow detection and tracking of hands brought into its proximity. The indicated detection error is small enough to prevent from interfering with normal operation in that case. Owing to the characteristic of azimuth detection, azimuth output reliability is generally lessened when the detected object is directly above the sensor. However, the proposed dome sensor can determine by elevation detection when the object is directly above the sensor, thus compensating for the shortcomings of azimuth detection. On the other hand, the detection distance is 60 mm in this paper. This is not enough to use in an actual application. Appropriate selection of the utilized elements or increase of arrangement density should help alleviate this problem.

The dome sensor developed in this research was designed for mounting into the grip of a robotic guide dog, but the proposed detection methods can be incorporated into other noncontact applications. For example, the rapid response features of the method can be applied to noncontact human interface applications (Fig. 15). Because the dome sensor can detect azimuths from the point of view of the sensor center, application to onscreen cursor manipulations should be straightforward. Furthermore, the dome sensor's elevation detection results in a 3D representation of the object, which should have applications to virtual reality research.

The proposed sensor uses discrete detection elements, allowing for adjustments to the internal resistor network to provide output best suited to the detection element layout. This lessens limitations on the form that detectors can take, allowing for mounting onto, for example, the side or end part of a device. Taking advantage of this freedom further expands the potential applications, such as allowing robots to acquire directional information about environmental objects from the point of view of any location on the robot's body.

V. Conclusion and Future Works

The present study developed a proximity sensor for simultaneous detection of azimuth and elevation. The features of the proposed dome sensor include rapid responsiveness and simpler wiring, while maintaining a 360° sensing range and detection from sensor sides to top. In future research, we plan to create more practical dome sensors with wider detection range on the same principle, and investigate potential applications.

References

[1] NSK Ltd. *Press Release: NSK Develops a Lead-Robot with Obstacle Avoidance Capabilities*. NSK Global, http://www.nsk.com/ company/presslounge/news/2011/press111027a.html, 2012-08-21.

[2] Zhiqiang Yu, Gao MEng, Huaping Liu, Xiaoyan Deng, Jianhua Liu, Qiurui Wu, Yuewei Liu, *Dynamic Obstacle Avoidance in Polar Coordinates for Mobile Robot Based on Laser Radar*, Computational Intelligence and Industrial Application, pp.334-338, 2008

[3] Kai-Tai Song, Shin-Yi Huang, *Mobile Robot Navigation Using Sonar Direction Weights*, Proc. IEEE Int. Conf. on Control Applications, Vol.2, pp.1073-1078, 2004

[4] Hyun-Don Kim, Jong-Suk Choi, Munsang Kim, Chang-Hoon Lee, *Reliable Detection of Sound' s Direction for Human Robot Interaction*, Proc. IEEE Int. Conf. on Intelligent Robots and Systems, Vol.3, pp.2411-2416, 2004

[5] Cheol-Taek Kim, Tae-Yong Choi, Byong Suk Choi, Ju-Jang Lee, *Robust Estimation of Sound Direction for Robot Interface*, Proc. IEEE Int. Conf. on Robotics and Automation, pp.3475-3480, 2008

[6] Sumit Badal, Srinivas Ravela, Bruce Draper, Allen Hanson, *A Practical Obstacle Detection and Avoidance System*, Application of Computer Vision, pp.97-104, 1994

[7] Dong Sung Kim, Young Shin Kim, Wook Hyun Kwon, *A Real Time Detection Algorithm Omnidirectional Image Sensors for Direction Error in for Mobile Robots*, Proc. IEEE Int. Conf. on Robotics and Automation, pp. 2982-2987, 1999

[8] Panagiotis Karras, Nikos Mamoulis, *Detecting the Direction of Motion in a Binary Sensor Network*, Proc. IEEE Int. Conf. on Sensor Network, Ubiquitous, and Trustworthly Computing, 2006

[9] K. Wohn, S. R. Maeng, *Pyramid-based Estimation of 2-D Motion for Object Tracking*, Proc. IEEE Int. Workshop on Intelligent Robots and Systems, Vol.2, pp.687-693, 1990

[10] Makoto Shimojo, Takuma Araki, Seiichi Teshigawara, Aiguo Ming, Masatoshi Ishikawa, *A Net-Structure Tactile Sensor Covering Free-form Surface and Ensuring High-Speed Response*, Proc. IEEE Int. conf. on Intelligent Robots and Systems, pp.670-675, 2007

[11] Hiroaki Hasegawa, Yoshitomo Mizoguchi, Kenjiro Tadakuma, Aiguo Ming, Masatoshi Ishikawa, Makoto Shimojo, *Development of Intelligent Robot Hand using Proximity, Contact and Slip sensing*, Proc. IEEE Int. Conf. on Robotics and Automation, pp.777-784, 2010

[12] Kazuki Terada, Yosuke Suzuki, Hiroaki Hasegawa, Satoshi Sone, Aiguo Ming, Masatoshi Ishikawa, Makoto Shimojo, *Development of Omni-Directional and Fast-Responsive Net-Structure Proximity Sensor*, Proc. IEEE Int. conf. on Intelligent Robots and Systems, pp.1954-1961, 2011